

Changes in the metabolome and microRNA levels in biological fluids might represent biomarkers of neurotoxicity: A trimethyltin study

Syed Z Imam¹, Zhen He¹, Elvis Cuevas¹, Hector Rosas-Hernandez¹, Susan M Lantz¹, Sumit Sarkar¹, James Raymick¹, Bonnie Robinson¹, Joseph P Hanig², David Herr³, Denise MacMillan³, Aaron Smith⁴, Serguei Liachenko¹, Sherry Ferguson¹, James O'Callaghan⁵, Diane Miller⁵, Christopher Soms⁶, Ingrid D Pardo⁶, William Slikker Jr¹, Jennifer B Pierson⁷, Ruth Roberts⁸, Binsheng Gong⁹, Weida Tong⁹, Michael Aschner¹⁰, Mary J Kallman¹¹, David Calligaro³ and Merle G Paule¹

¹Division of Neurotoxicology, US FDA, NCTR, Jefferson, AR 72079, USA; ²US FDA CDER, MD 20993, USA; ³US EPA, NHEERL, Research Triangle Park, North Carolina, NC 27711, USA; ⁴Lilly, Lilly Corporate Center, Indianapolis, Indiana, IN 46285, USA; ⁵CDC-NIOSH, Morgantown, WV 26505-2888, USA; ⁶Pfizer, Groton, Connecticut, CT 06340, USA; ⁷ILSI-HESI, Washington, DC 20005, USA; ⁸Department of Biosciences, University of Birmingham, Birmingham B15 2TT, UK; ⁹Division of Bioinformatics, US FDA, NCTR, Jefferson, AR 72079, USA; ¹⁰Albert Einstein College of Medicine, Bronx, NY 10461, USA; ¹¹Kallman Preclinical Consulting, Greenfield, IN 46140, USA

Corresponding author: Syed Z Imam. Email: Syed.Imam@fda.hhs.gov

Impact statement

These data will help design follow-on studies with other known neurotoxins to be used to assess the broad applicability of the present findings. Together this approach represents an effort to begin to develop and qualify a set of translational biochemical markers of neurotoxicity that will be readily accessible in humans. Such biomarkers could prove invaluable for drug development research ranging from pre-clinical studies to clinical trials and may prove to assist with monitoring of the severity and life cycle of brain lesions.

Abstract

Neurotoxicity has been linked with exposure to a number of common drugs and chemicals, yet efficient, accurate, and minimally invasive methods to detect it are lacking. Fluid-based biomarkers such as those found in serum, plasma, urine, and cerebrospinal fluid have great potential due to the relative ease of sampling but at present, data on their expression and translation are lacking or inconsistent. In this pilot study using a trimethyl tin rat model of central nervous system toxicity, we have applied state-of-the-art assessment techniques to identify potential individual biomarkers and patterns of biomarkers in serum, plasma, urine or cerebral spinal fluid that may be indicative of nerve cell damage and degeneration. Overall changes in metabolites and microRNAs were observed in biological fluids that

were associated with neurotoxic damage induced by trimethyl tin. Behavioral changes and magnetic resonance imaging T₂ relaxation and ventricle volume changes served to identify animals that responded to the adverse effects of trimethyl tin.

Keywords: Bioimaging, biomarkers, brain, neurobiology, neurotoxicology, translational

Experimental Biology and Medicine 2018; 243: 228–236. DOI: 10.1177/1535370217739859

Introduction

Neurotoxic effects resulting from drug and other chemical exposures pose significant public health problems. For example, in the drug development community, neurotoxicity accounts for 25% of the adverse effects seen during clinical trials.¹ Environmental toxicants such as mercury, manganese, pesticides, together with contaminants in

designer drugs of abuse such as 1-methyl-4-phenyl-1,2,3,6-tetrahydropyridine (MPTP) and a growing inventory of industrial chemicals have been linked to neurological damage and neurodegenerative disease.² Understanding the long-term cognitive deficits and related biochemical derangements seen after exposure to general anesthetics,³ the proinflammatory cytokine-mediated neurotoxicity that

occurs with some chemotherapies,⁴ the neurotoxicity induced by antiretroviral agents⁵ and the neurotoxicity associated with general drug development efforts would benefit greatly from the use of a readily available fluidic biomarker(s) of neurotoxicity. Traditionally, neurotoxicity has been assessed preclinically using composite data sets including functional assessments and traditional histopathological examinations. There are, however, many shortcomings with this approach that are evidenced by the high percentage of clinical trial failures attributable to adverse effects on the nervous system which were not identified in pre-clinical investigations. One of the major problems is that the relevant observations are typically made over a very limited time course. Histopathologic analyses often suffer from inadequate spatial sampling and are invasive which can lead to statistical challenges and lack of longitudinal measurements.⁶ Functional metrics may be masked by reserve capacity, large variability, or lack of connection to underlying pathology.⁶

The International Life Sciences Institute (ILSI) – Health and Environmental Sciences Institute (HESI), a non-profit, science-driven organization developed a plan to identify biomarkers associated with the onset, severity, and progression of neurotoxic insult.² The prioritization of this work was an acknowledgment that neurotoxicity poses a significant challenge that can benefit from a “big science,” collaborative approach to search for detectable biomarkers. An expanding scientific literature is providing evidence that highlights the potential utility of fluid-based biomarkers of neurotoxicity.^{7,8} Similarly, neuroimaging approaches also present significant advantages for identifying potential biomarkers of neurotoxicity because they are less invasive than other procedures and, like biofluids, provide the opportunity to assess subjects repeatedly over time.^{9,10} For this pilot study, a diverse group of experts (part of the ILSI-HESI Committee on Translational Biomarkers of Neurotoxicity) reviewed existing methods and approaches and assessed the challenges and opportunities for identifying novel biomarkers associated with neurotoxicity. The group identified fluidic biomarkers to be assessed alongside MRI endpoints with the intent to link them to traditional behavioral endpoints.² In the present *in vivo* study, the prototypical neurotoxicant TMT was used in the rat as a denervation tool to generate significant CNS insult. The selection of TMT was based on previous extensive dose and time course analyses of neurotoxicological biomarkers from studies in which the hippocampus was the focus because its damage is easily visible using Nissl stain.^{11,12} Subsequently, a search for biomarkers that may be related to neurotoxicity in biological fluids was undertaken. The primary fluidic biomarkers identified included brain-abundant microRNAs (miRNAs) and a group of biomolecules representing changes in the metabolome. Continuing analyses are underway to further mine the data to clarify the correlations between members of specific families of circulating biomarkers with histopathological endpoints of neurotoxicity that served as the phenotypic anchor for all observations. It is hoped that further validation of the current findings will lead to a formal process of biomarker qualification according to Food and Drug

Administration (FDA) guidance¹³ with the goal of increasing the likelihood that the identified biomarkers will be broadly employed.

Materials and methods

Adult male Sprague Dawley rats (Taconic, Inc.) were allocated to groups ($n = 12$ per group per sacrifice time). All procedures with animals were carried out according to the National Institutes of Health Guide for the Care and Use of Laboratory Animals. The animal protocol was approved by the National Center for Toxicological Research (NCTR)/FDA Institutional Animal Care and Use Committee. To monitor overt behavioral aspects of TMT effects, the locomotor activity of each animal was assessed during a 30-min session prior to the terminal MRI and sacrifice. Baseline MRIs were obtained from all animals prior to TMT (one i.p. injection of 7 mg/kg) or vehicle (saline) exposure. Behavioral observations, and MRI scans and tissue samples were obtained at 2 ($n = 11/12$ for TMT), 6 ($n = 10/12$ for TMT), 10 ($n = 6/12$ for TMT), or 14 ($n = 5/12$ TMT) days post-treatment. The n for control groups at all time points was 12 and all controls survived throughout the experiment except on post-treatment day 6 ($n = 11$) when one animal succumbed to anesthesia during MRI imaging. Tissue samples were collected at each time point from isoflurane anesthetized animals and included brain, plasma, serum, CSF, and urine. Samples were kept frozen at -80°C until analysis with the specific goal of identifying key biomolecules associated with the expression of frank neurotoxicity.

Locomotor activity was measured using open field apparatus as previously described.¹⁴ Each rat was placed into a Plexiglas chamber for 30 min the morning of sacrifice (i.e. 2, 6, 10, and 14 days post-treatment). Horizontal and vertical (rearing) activities were automatically recorded via a 16×16 array of photobeams (PAS-Open Field, San Diego Instruments, San Diego, CA) interfaced with a computer. Endpoints included total horizontal activity (sum of lower beam breaks/session) and total vertical activity (sum of upper beam breaks/session).

Targeted metabolomic analyses of cerebrospinal fluid (CSF), plasma, serum, and urine samples were conducted at the National Health and Environmental Effects Research Laboratory (NHEERL, Research Triangle Park, North Carolina) using an AbsoluteIDQTM p180 kit from Biocrates Life Sciences (Innsbruck, Austria) which generates a mass spectrometry (MS)-based analysis of up to 186 metabolites of different classes (acylcarnitines, amino acids, hexoses, biogenic amines, glycerophospholipids, and sphingolipids). Analyses were performed according to kit instructions using an AB Sciex (Framingham, MA) 4000 Qtrap linear ion trap mass spectrometer. Samples (10–30 μL) were derivatized and extracted in 96-well plates.¹⁵ To obtain adequate sample volumes for the metabolome analyses, two to four CSF samples from the same sacrifice group were combined. This resulted in three samples per group at each sacrifice time. Samples were analyzed using one method (FIA/MS/MS) for lipids and hexoses and using a second method (LC/MS/MS) for

amino acids and biogenic amines. Analytes were quantitated using multiple reaction monitoring transitions and internal standards. Raw data were reviewed and processed using AB Sciex Analyst (version 1.5.2) software. Data were loaded into Biocrates MetIDQ (Boron version) software for plate QC validation. Analyte levels were compared to controls using Welch's unequal variance *t*-test. Only analytes that were significantly ($p < 0.05$) different from concurrent controls are reported. The log₂ fold change (treated/control mean) was calculated and graphed for the significantly altered analytes.

For the miRNA analyses, quantitative polymerase chain reactions (qPCR) were performed on 78 CSF samples and 79 serum samples; 15 μ l of CSF and 50 μ l of serum were subjected to total RNA isolation using the miRNeasy™ kit from Qiagen (217004, Valencia CA). All samples of a lower volume were brought up to 50 μ l with water and 5 μ l of 200 nM cel-miR-55 were spiked into 50 μ l of CSF and serum after addition of Qiazol. RNAs were eluted in 80 μ l of 95°C H₂O and reverse transcription was executed using the miRCURY LNA miRNA Universal cDNA Synthesis Kit (203301, Exiqon). A reverse transcription dilution series was employed to assess the impact of carryover PCR inhibition from the primary sample matrix. For this test, primary total RNA isolates from a select set of serum samples were diluted 1:2, 1:4, and 1:10 and then assayed against the cel-miR-55 spike in control; the resulting PCR curves were assessed for increased sensitivity vs dilution. A 1:4 dilution of primary RNA from both plasma and serum proved optimal for mitigating PCR inhibition while preserving target sensitivity. Five μ l of the extracted RNAs, diluted 1:4, were then used in 20 μ l reverse transcriptase (RT) reactions. A no template control (NTC) and two -RT controls were also included. Pre-amplification for CSF and serum sample analysis was necessary due to both the limited volume of available sample and limited target concentration. CSF and serum samples were pre-amplified following the Exiqon miRNA Pre-Amp protocol: 2.5 μ l of RT product were used for each sample type for a total reaction volume of 25 μ l. Samples were diluted 1:20 immediately prior to qPCR in a 96-deep well plate by combining 25 μ l of RT product and 475 μ l of water. Exiqon miRCURY LNA assays and ExiLent SYBR Green Master Mix (203421, Exiqon) were utilized for PCR; 4 μ l of cDNA was used for a total reaction volume of 20 μ l. Data were collected on a 7900HT sequence detection system (4351405, Life Technologies) and miRNA levels were compared to controls using Welch's unequal variance *t*-test. Only those that were significantly ($p < 0.05$) different from concurrent controls are reported.

For the MRI scans, rats underwent imaging before TMT/vehicle exposure and on days 2, 6, 10, or 14 after exposure. MRI was performed using a Bruker BioSpec 7T/30 system employing a bird-cage transmit and a 4-channel phased array rat brain-optimized receive coil.¹⁶ Animals were anesthetized using isoflurane general anesthesia (3% induction, 1–2% maintenance in 1 L/min oxygen) and body temperature was maintained at $37.0 \pm 0.5^\circ\text{C}$ for the duration (~45 min). The MRI protocol consisted of anatomical scout imaging and T₂ mapping. Whole brain T₂ relaxation mapping was performed using a multi-echo, spin

echo sequence (FOV = $3.84 \times 3.84 \times 2.4$ cm, matrix $192 \times 192 \times 24$, 16 echoes with 15 ms spacing, TR = 6 s, NA = 1). MRI T₂ maps were produced from original multi-echo images using pixel-by-pixel simple exponential fitting.⁹ T₂ maps were skull-stripped and the number of voxels with values higher than 120 ms in manually segmented lateral ventricle areas was calculated, which represented the lateral ventricle volume in the brain as T₂ of CSF is much higher than that of the brain parenchyma. Statistical analysis of ventricular volume changes was performed using a paired *t*-test.

Results

Profiles of 29 brain-enriched miRNAs were obtained to determine whether brain-enriched miRNAs observable in CSF and serum showed toxicity-related changes. Large changes in a variety of miRNAs were observed in the CSF: a ~3.5-fold increase was seen in the expression of miR-218a-5p at day 14, which typically has its largest expression in the hippocampus (Figure 1(a)). Additionally in the CSF, miR-9a-3p and 5p showed significant alterations at days 6 and 10 and 2 and 14, respectively (Figure 1(b) and (c)). In serum, miRNAs 125b-5p, 138-5p, and 221-3p showed small increases at day 6; however, a decrease was seen on days 2 and 10 for 221-3p and day 10 for 138-5p (Figure 1(d) to (f)).

Metabolite changes were observed in CSF, plasma, and urine. Metabolite classes included acylcarnitines, amino acids, biogenic amines, hexoses, phosphatidylcholines, lyso-phosphatidylcholines, and sphingomyelins. In CSF, increases in acylcarnitines, phosphatidylcholines, biogenic amines, and sphingolipids at two and six days were noted and increases in amino acids were observed at all time points after treatment (Figure 2(a)). In plasma, there were increased levels of acylcarnitines, phosphatidylcholines, amino acids, and sphingolipids at two and six days (Figure 2(b)). Increased levels of acylcarnitines in urine at two and six days (Figure 2(c)) were very similar to the changes noted in CSF and plasma. Very few significant increases in acylcarnitines were observed in the serum metabolome (Figure 2(d)).

For locomotor activity, ANOVAs indicated significant interactions of treatment by number of days post-treatment for total horizontal activity and total vertical activity. Relative to the control group, the TMT-treated group exhibited significantly decreased horizontal activity at 6 days post-treatment, but increased activity at 10 days post-treatment (Figure 3).

MRI showed significant increases in CSF volumes in the lateral ventricles of TMT-treated rats without significant edema, as only few animals showed detectable increases of T₂ relaxation values in the hippocampus (Figure 4).

Discussion

Our findings suggest that TMT induced significant changes in energy metabolism and damage to mitochondria and membranes, presumably in the CNS as no or minimal toxicities were observed in any other tissue examined (liver,

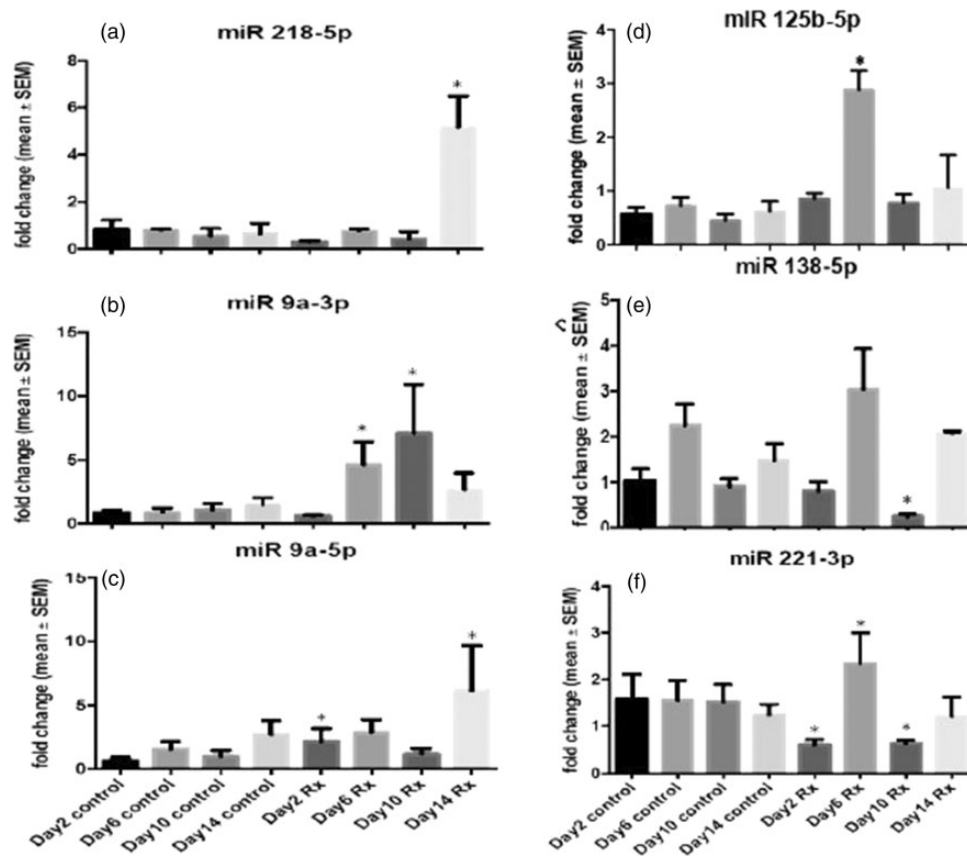


Figure 1. miRNA profiles in CSF (a–c) and serum (d–f) of adult male rats 2, 6, 10, and 14 days after a single dose of TMT. miRNA levels were compared to controls using Welch's unequal variance t-test. Only those that were significantly ($P < 0.05^*$) different from concurrent controls are reported.

kidney, thymus, adrenal, and sciatic nerve, data not shown). Biological markers of these effects were reflected in bodily fluids as well as brain tissue. It remains to be determined if plasma and urine markers identified here will consistently mirror CSF markers of frank CNS neuropathology (cell death). If this is the case then they may serve as useful, readily accessible surrogates of neurotoxicity.

Identifying biomarkers relevant to neurotoxicity is vital for developing tools to monitor adverse nervous system events. Appropriate molecular and physiological biomarkers should serve as predictive indicators of neurotoxicity. The present results demonstrate that a major neurotoxic event, exposure to TMT, can result in significant alterations in the metabolome and miRNA expression, all of which likely play roles in neuronal function. Such fluidic changes were accompanied by typical TMT-induced behavioral changes and MRI signals.

miRNAs are valuable biomolecules because of their stability and, thus, detectability. Their non-antibody-based detection and their stability in bodily fluids facilitate their translational utility^{17–19} and there are several sensitive detection methods available for the identification of pathological miRNAs.²⁰ A recent study showed that different miRNA expression patterns are associated with specific MRI measures that are characteristic of the different stages and severity of multiple sclerosis and, thus, can serve as surrogate markers of disease progression.²¹ In the present study, hippocampus-specific miR-218a-5p was

significantly increased in CSF after TMT exposure. miR-218a-5p is enriched in the brain with its highest expression occurring in the hippocampus, cortex, and cerebellum. There is some expression in the duodenum and minimal expression in the kidney.²² A recent study has shown that CSF levels of miR-218 correlated with the motor neuron loss in models of amyotrophic lateral sclerosis (ALS) suggesting that it may be a clinically useful marker of ALS progression.²³ Our observation of miR-218a-5p increases in CSF after TMT-induced neurotoxicity supports the notion that it is a biomarker for CNS neurotoxicity. The miR-9 family is highly expressed in both the developing and adult vertebrate brain and participates in neuronal progenitor maintenance, neurogenesis and neuron differentiation.²⁴ A recent study has shown that miR-9-5p/3p are integral to the regulation of brain development and their derangement has been implicated in several neurological disorders: it has been suggested that miR-9-3p regulates synaptic plasticity and memory.²⁵ In the present study, miR-9a-3p and -5 were elevated in CSF at varying times after TMT exposure. In addition, significant changes were observed in a few miRNAs in serum after TMT-exposure: the relevance of those miRNAs to neuronal health has yet to be established.

The metabolomic analysis presented here included a large list of metabolites representing many physiological processes. Such a wide range of metabolites is likely to represent the overall metabolic profile of the whole animal. It is important to note that pathology was not observed in the

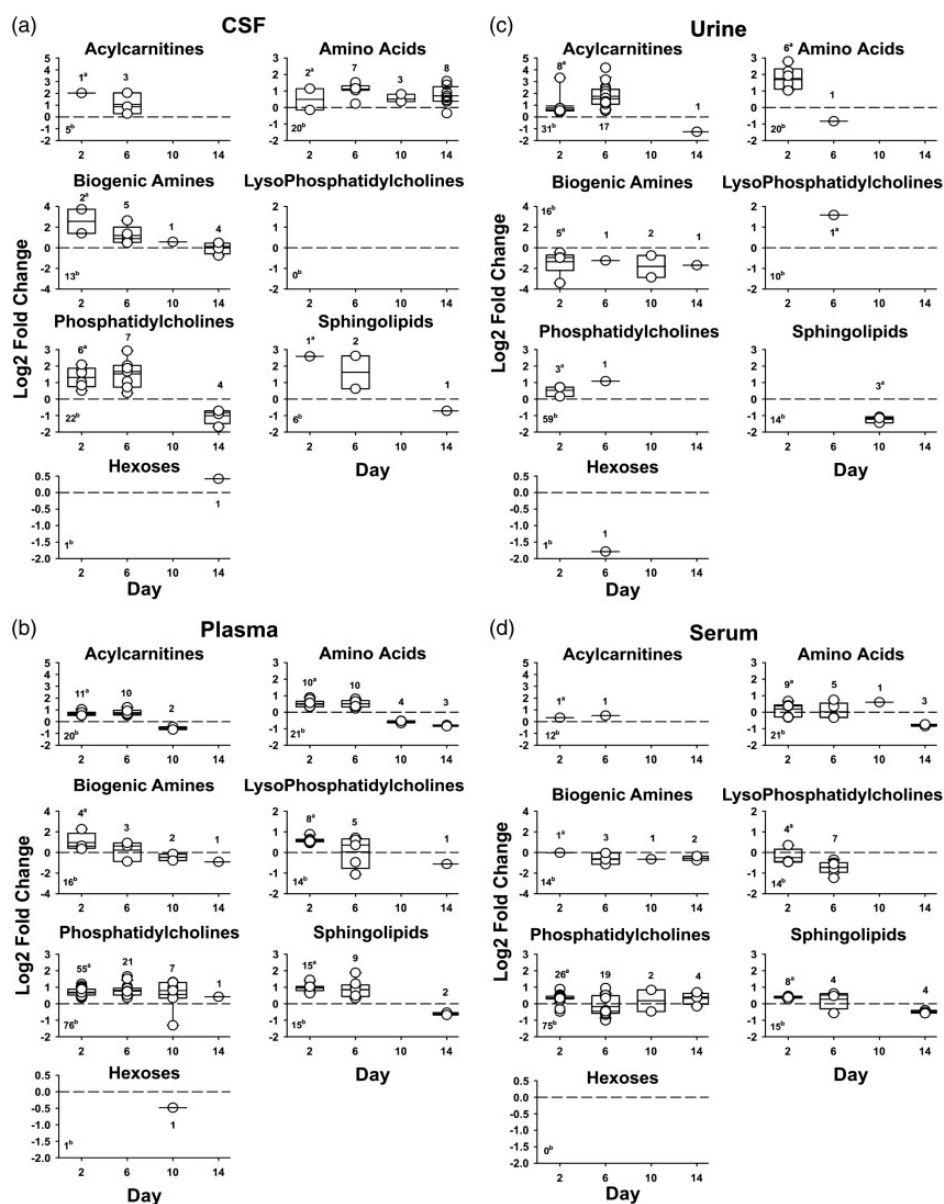


Figure 2. Metabolite levels in CSF (a), plasma (b), urine (c) and serum (d) of adult male rats 2, 6, 10, and 14 days after a single dose of TMT. Analyte levels were compared to controls using Welch's unequal variance *t*-test. Only analytes that were significantly ($p < 0.05$) different from concurrent controls on each day are reported. The log2 fold change (treated/control mean) was calculated and graphed for the significantly altered analytes (a = number of metabolites significantly altered; b = number of metabolites detected within the range of quantitation, all sugars were grouped as a singular hexose metabolite).

periphery in organs included the liver, kidney, thymus, adrenal, and sciatic nerve. While not definitive, these findings suggest that observed changes in metabolic profiles reflect responses to CNS toxicity. It is important to note that the results of the metabolomic analysis are presented in terms of "classes" of metabolites to assist with interpreting which large scale processes may have been altered by TMT. However, findings for individual metabolites (some of which could be generated by multiple pathways) are available for analysis. Collectively, the observed metabolomic changes suggest alterations in energy metabolism and mitochondrial and membrane damage, presumably in the central nervous system.

When quantifying biomarkers such as these metabolomic measures, interpretation of observed changes should

be made after considerations of criteria such as those described in the modified Bradford-Hill criteria.^{26,27} These criteria include: (1) are the changes dose-related? (not addressed in the present study); (2) do the changes correlate with the time-course of toxicity? (yes in this study, changes in the metabolome were observed that correlated with the time-course of other measures of neurotoxicity); (3) if the toxicity is blocked, are the metabolomic changes reversible? (this was not addressed in the current study); and (4) are the changes biologically plausible – are the changes in the metabolome consistent with what is known about the mechanism of toxicity? (at least partially yes in the present study, the metabolic changes are consistent with degeneration of cells, membranes, and altered mitochondrial respiration). Thus, the changes in

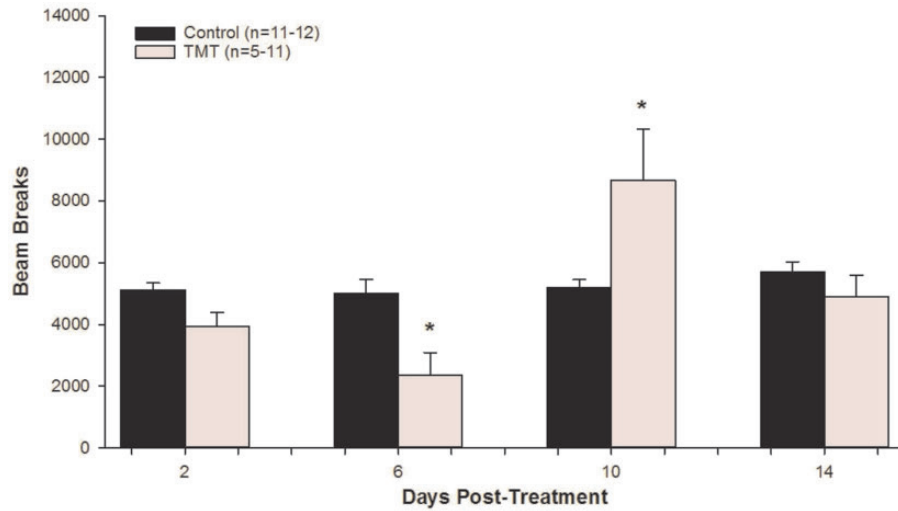


Figure 3. Locomotor activity as measured by photo-beam breaks of adult male rats 2, 6, 10, and 14 days after a single dose of TMT. *Post hoc* comparisons of the significant interaction of treatment (saline vs. TMT) and days post-treatment indicated that the saline and TMT groups differed significantly at day 6 only.

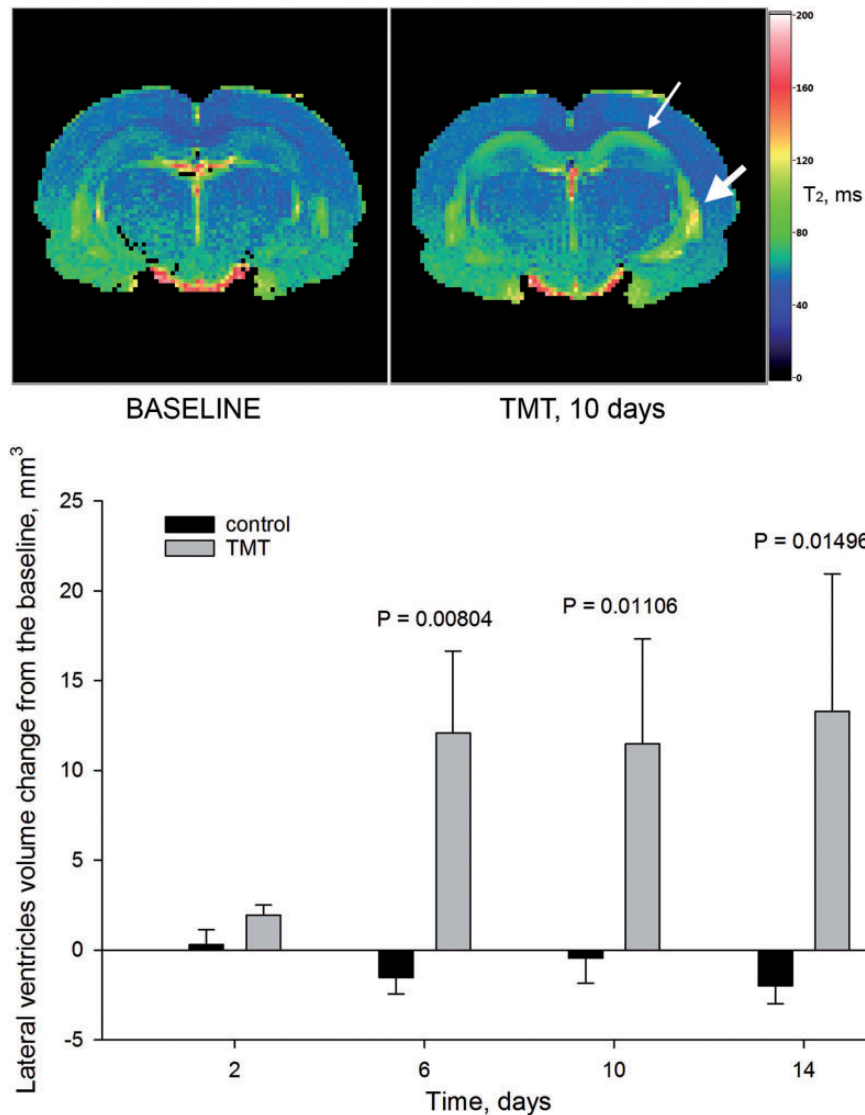


Figure 4. An example of a T_2 relaxation map (top panel, single slice out of 24) of one TMT-treated animal (at baseline and after TMT treatment) shows both a T_2 increase in the dorsal hippocampus (small arrow) as well as an increase in the volume of the lateral ventricle (large arrow). The bar graph (bottom panel) shows averaged changes in the lateral ventricle volumes in rats after 2, 6, 10, and 14 days after TMT treatment. *P* value represents the statistical significance of difference between control and TMT groups. Data are Means \pm S.E.Ms.

the fluid metabolome reported here are consistent with TMT-induced neurotoxicity within the framework of the current study. Clearly, additional work is necessary to more directly link these alterations in metabolomic markers to neurotoxicity and to identify possible contributions from other tissue/cell types.

The observation that TMT-induced time-dependent changes in the levels of acylcarnitines in CSF, plasma, serum, and urine clearly shows that they are correlated with TMT-induced changes in brain and that they may represent early signals of CNS damage. Brain acylcarnitines play major roles in the maintenance of mitochondrial function and cholinergic transmission²⁸ and neuronal acylcarnitines provide antioxidant support and contribute to membrane integrity via their role in lipid biosynthesis.²⁹ The increase in CSF acylcarnitine levels at the earlier time points after TMT administration might suggest an attempt to boost cellular defense mechanisms that subsequently drop as cells die at later time points. The pattern of acylcarnitine levels observed in the CSF is also reflected in plasma and urine, thereby suggesting that fluid levels of acylcarnitines are correlated with the neurotoxic response to TMT.

Changes in brain levels of amino acids noted in the present study suggest changes in various physiological functions including energy production, neurotransmitter regulation, and cellular architecture.³⁰ In the present study, there was a persistent increase in amino acid levels in CSF over the 14 days of observation but a time-dependent decline in serum, plasma and urine levels. This observation might be indicative of transport of amino acids from the periphery into the CNS or an alteration of amino acid metabolism in the CNS itself.

Phospholipids and sphingolipids form integral components of cellular membranes and lipoproteins^{31,32} and neuronal membrane integrity is critical for inter- and intra-neuronal communication. Changes in these membrane constituents likely accompany neurodegenerative changes,³³ which have been reported as early as two days after treatment with TMT.¹¹ Thus, it is important to note that these changes in the metabolome were in concordance with some of the earliest reported neuronal toxicity produced by TMT.

MRI techniques represent significant advances in the diagnosis and monitoring of neurological disease.^{34,35} Imaging techniques, especially MRI, provide tools for differentiating among heterogeneous pathologic processes: they can be used to evaluate axonal and neuronal loss and progressive neurodegenerative processes and to link physical brain damage with cognitive impairment.^{36,37} In the present studies, the neurotoxic damage induced by TMT was employed as a phenotypic anchor to which fluidic biomarkers and alterations in MRI signals can be tied: TMT-induced neurotoxicity that resulted in alterations in fluidic metabolomic markers and brain-enriched miRNAs also produced significant increase in lateral ventricular volume in all impaired rats without the development of any edema; T_2 relaxation measures were also affected in the hippocampus. Enlarged ventricles observed after TMT exposure have also been reported previously but they were described in terms of decreases in the volume

of the neuropil as evident morphologically by loss of weight of the hippocampus after TMT exposure.¹² Increases in ventricular volumes that might represent a loss of hippocampal neuropil may be independent of blood-brain barrier (BBB) damage, as TMT has not been reported to induce significant BBB damage around the onset of neuropathology during TMT-induced neurotoxic damage.³⁸

Although the present studies are preliminary, they provide solid platforms from which to search for minimally invasive neuronal and bio-fluid-based biomarkers of neurotoxic damage after CNS insult. It is hoped that future studies based on these current findings will reveal specific circulating biomarkers related to the extent of neurotoxic damage. Such biomarkers would be beneficial during drug development, injury assessments and diagnoses, and therapeutic monitoring.

Disclaimer

The opinions presented here are those of the authors. No official support or endorsement by the US Food and Drug Administration or the US Environmental Protection Agency or the National Institute for Occupational Safety and Health is intended or should be inferred.

Authors' contributions: All authors participated in the design, interpretation of the studies and analysis of the data and review of the manuscript; SZM, ZH, EC, HR-H, SML, SS, JR, BR conducted the experiments and contributed to data analyses; JPH, DH, DMc, AS, SL, SF, JO, DM, CS, IDP, WS, BG, WT contributed to data analyses and interpretation; RR, DC, MGP, JBP, MJK, MA contributed to data analyses, interpretation and provided additional intellectual support throughout the study. SZM, MGP, DC, RR, JBP, CS contributed to the drafting and editing of the manuscript.

ACKNOWLEDGMENTS

The authors wish to express their gratitude to the HESI Committee on Translational Biomarkers of Neurotoxicity members for supporting the efforts of this collaborative project. Additionally, the authors would like to thank Drs. John Talpos and Annie Lumen for their thorough review of the manuscript.

DECLARATION OF CONFLICTING INTERESTS

HESI's scientific initiatives are primarily supported by the in-kind contributions (from public and private sector participants) of time, expertise, and experimental effort. These contributions are supplemented by direct funding (that primarily supports program infrastructure and management) provided primarily by HESI's corporate sponsors.

FUNDING

The study was supported by NCTR/FDA protocol number E0758001.

REFERENCES

1. Cook D, Brown D, Alexander R, March R, Morgan P, Satterthwaite G, Pangalos MN. Lessons learned from the fate of AstraZeneca's drug pipeline: a five-dimensional framework. *Nat Rev Drug Discov* 2014;**13**:419-31
2. Roberts RA, Aschner M, Calligaro D, Guilarte TR, Hanig JP, Herr DW, Hudzik TJ, Jeromin A, Kallman MJ, Liachenko S, Lynch JJ, 3rd, Miller DB, Moser VC, O'callaghan JP, Slikker W, Jr, Paule MG. Translational biomarkers of neurotoxicity: a health and environmental sciences institute perspective on the way forward. *Toxicol Sci* 2015;**148**:332-40
3. Fodale V, Tripodi VF, Penna O, Fama F, Squadrito F, Mondello E, David A. An update on anesthetics and impact on the brain. *Expert Opin Drug Saf* 2017;**16**:997-1008
4. Vitali M, Ripamonti CI, Roila F, Proto C, Signorelli D, Imbimbo M, Corrao G, Brissa A, Rosaria G, de Braud F, Garassino MC, Russo GL. Cognitive impairment and chemotherapy: a brief overview. *Crit Rev Oncol Hematol* 2017;**118**:7-14
5. Stauch KL, Emanuel K, Lamberty BG, Morsey B, Fox HS. Central nervous system-penetrating antiretrovirals impair energetic reserve in striatal nerve terminals. *J Neurovirol Epub ahead of print* 2017. doi: 10.1007/s13365-017-0573-5.
6. Bolon B, Garman RH, Pardo ID, Jensen K, Sills RC, Roulois A, Radovsky A, Bradley A, Andrews-Jones L, Butt M, Gumprecht L. STP position paper: recommended practices for sampling and processing the nervous system (brain, spinal cord, nerve, and eye) during nonclinical general toxicity studies. *Toxicol Pathol* 2013;**41**:1028-48
7. Koh W, Pan W, Gawad C, Fan HC, Kerchner GA, Wyss-Coray T, Blumenfeld YJ, El-Sayed YY, Quake SR. Noninvasive in vivo monitoring of tissue-specific global gene expression in humans. *Proc Natl Acad Sci U S A* 2014;**111**:7361-6
8. Guo D, Liu J, Wang W, Hao F, Sun X, Wu X, Bu P, Zhang Y, Liu Y, Zhang Q, Jiang F. Alteration in abundance and compartmentalization of inflammation-related miRNAs in plasma after intracerebral hemorrhage. *Stroke* 2013;**44**:1739-42
9. Hanig J, Paule MG, Ramu J, Schmued L, Konak T, Chigurupati S, Slikker W, Jr, Sarkar S, Liachenko S. The use of MRI to assist the section selections for classical pathology assessment of neurotoxicity. *Regul Toxicol Pharmacol* 2014;**70**:641-7
10. Liachenko S, Ramu J, Konak T, Paule MG, Hanig J. Quantitative assessment of MRI T2 response to kainic acid neurotoxicity in rats in vivo. *Toxicol Sci* 2015;**146**:183-91
11. Balaban CD, O'callaghan JP, Billingsley ML. Trimethyltin-induced neuronal damage in the rat brain: comparative studies using silver degeneration stains, immunocytochemistry and immunoassay for neuronotypic and gliotypic proteins. *Neuroscience* 1988;**26**:337-61
12. Brock TO, O'callaghan JP. Quantitative changes in the synaptic vesicle proteins synapsin I and p38 and the astrocyte-specific protein glial fibrillary acidic protein are associated with chemical-induced injury to the rat central nervous system. *J Neurosci* 1987;**7**:931-42
13. Woodcock J, Buckman S, Goodsaid F, Walton MK, Zineh I. Qualifying biomarkers for use in drug development: a US Food and Drug Administration overview. *Expert Opin Med Diagn* 2011;**5**:369-74
14. Ferguson SA, Law CD, Sarkar S. Chronic MPTP treatment produces hyperactivity in male mice which is not alleviated by concurrent trehalose treatment. *Behav Brain Res* 2015;**292**:68-78
15. Moser VC, Stewart N, Freeborn DL, Crooks J, MacMillan DK, Hedge JM, Wood CE, McMahan RL, Strynar MJ, Herr DW. Assessment of serum biomarkers in rats after exposure to pesticides of different chemical classes. *Toxicol Appl Pharmacol* 2015;**282**:161-74
16. Imam SZ, Lantz-McPeak SM, Cuevas E, Rosas-Hernandez H, Liachenko S, Zhang Y, Sarkar S, Ramu J, Robinson BL, Jones Y, Gough B, Paule MG, Ali SF, Binienda ZK. Iron oxide nanoparticles induce dopaminergic damage: in vitro pathways and in vivo imaging reveals mechanism of neuronal damage. *Mol Neurobiol* 2015;**52**:913-26
17. Ebert MS, Sharp PA. Roles for microRNAs in conferring robustness to biological processes. *Cell* 2012;**149**:515-24
18. Haghighi A, Haghighi A, Hellwig K, Baraniskin A, Holzmann A, Decard BF, Thum T, Gold R. Regulated microRNAs in the CSF of patients with multiple sclerosis: a case-control study. *Neurology* 2012;**79**:2166-70
19. Mitchell PS, Parkin RK, Kroh EM, Fritz BR, Wyman SK, Pogosova-Agadjanyan EL, Peterson A, Noteboom J, O'brian KC, Allen A, Lin DW, Urban N, Drescher CW, Knudsen BS, Stirewalt DL, Gentleman R, Vessella RL, Nelson PS, Martin DB, Tewari M. Circulating microRNAs as stable blood-based markers for cancer detection. *Proc Natl Acad Sci USA* 2008;**105**:10513-8
20. Mestdagh P, Hartmann N, Baeriswyl L, Andreasen D, Bernard N, Chen C, Cheo D, D'andrade P, DeMayo M, Dennis L, Derveaux L, Feng Y, Fulmer-Smentek S, Gerstmayer B, Gouffon J, Grimley C, Lader E, Lee KY, Luo S, Mouritzen P, Narayanan A, Patel S, Peiffer S, Ruberg S, Schroth G, Schuster D, Shaffer JM, Shelton EJ, Silveria S, Ulmanella U, Veeramachaneni V, Staedtler F, Peters T, Guettouche T, Wong L, Vandesompele J. Evaluation of quantitative miRNA expression platforms in the microRNA quality control (miRQC) study. *Nat Meth* 2014;**11**:809-15
21. Regev K, Healy BC, Khalid F, Paul A, Chu R, Tauhid S, Tummala S, Diaz-Cruz C, Raheja R, Mazzola MA, von Glehn F, Kivisakk P, Dupuy SL, Kim G, Chitnis T, Weiner HL, Gandhi R, Bakshi R. Association between serum MicroRNAs and magnetic resonance imaging measures of multiple sclerosis severity. *JAMA Neurol* 2017;**74**:275-85
22. Ludwig N, Leidinger P, Becker K, Backes C, Fehlmann T, Pallasch C, Rheinheimer S, Meder B, Stahler C, Meese E, Keller A. Distribution of miRNA expression across human tissues. *Nucleic Acids Res* 2016;**44**:3865-77
23. Hoye ML, Koval ED, Wegener AJ, Hyman TS, Yang C, O'brien DR, Miller RL, Cole T, Schoch KM, Shen T, Kunikata T, Richard JP, Gutmann DH, Maragaski NJ, Kordasiewicz HB, Dougherty JD, Miller TM. MicroRNA profiling reveals marker of motor neuron disease in ALS models. *J Neurosci* 2017;**37**:5574-86
24. Radhakrishnan B, Alwin Prem Anand A. Role of miRNA-9 in brain development. *J Exp Neurosci* 2016;**10**:101-20
25. Sim SE, Lim CS, Kim JI, Seo D, Chun H, Yu NK, Lee J, Kang SJ, Ko HG, Choi JH, Kim T, Jang EH, Han J, Bak MS, Park JE, Jang DJ, Baek D, Lee YS, Kaang BK. The brain-enriched MicroRNA miR-9-3p regulates synaptic plasticity and memory. *J Neurosci* 2016;**36**:8641-52
26. Hill AB. The environment and disease: association or causation? *Proc R Soc Med* 1965;**58**:295-300
27. Meek ME, Palermo CM, Bachman AN, North CM, Jeffrey Lewis R. Mode of action human relevance (species concordance) framework: evolution of the Bradford Hill considerations and comparative analysis of weight of evidence. *J Appl Toxicol* 2014;**34**:595-606
28. McGill MR, Li F, Sharpe MR, Williams CD, Curry SC, Ma X, Jaeschke H. Circulating acylcarnitines as biomarkers of mitochondrial dysfunction after acetaminophen overdose in mice and humans. *Arch Toxicol* 2014;**88**:391-401
29. Jones LL, McDonald DA, Borum PR. Acylcarnitines: role in brain. *Prog Lipid Res* 2010;**49**:61-75
30. Wu G. Amino acids: metabolism, functions, and nutrition. *Amino Acids* 2009;**37**:1-17
31. Cole LK, Vance JE, Vance DE. Phosphatidylcholine biosynthesis and lipoprotein metabolism. *Biochim Biophys Acta* 2012;**1821**:754-61
32. Hermansson M, Hokynar K, Somerharju P. Mechanisms of glycerophospholipid homeostasis in mammalian cells. *Prog Lipid Res* 2011;**50**:240-57
33. Farooqui AA, Horrocks LA, Farooqui T. Glycerophospholipids in brain: their metabolism, incorporation into membranes, functions, and involvement in neurological disorders. *Chem Phys Lipids* 2000;**106**:1-29
34. Filippi M, Rocca MA, Arnold DL, Bakshi R, Barkhof F, De Stefano N, Fazekas F, Frohman E, Wolinsky JS. EFNS guidelines on the use of neuroimaging in the management of multiple sclerosis. *Eur J Neurol* 2006;**13**:313-25
35. Filippi M, Wolinsky JS, Comi G, Group CS. Effects of oral glatiramer acetate on clinical and MRI-monitored disease activity in patients with relapsing multiple sclerosis: a multicentre, double-blind, randomised, placebo-controlled study. *Lancet Neurol* 2006;**5**:213-20

36. Sanfilipo MP, Benedict RH, Sharma J, Weinstock-Guttman B, Bakshi R. The relationship between whole brain volume and disability in multiple sclerosis: a comparison of normalized gray vs. white matter with misclassification correction. *Neuroimage* 2005;**26**:1068–77
37. Sanfilipo MP, Benedict RH, Weinstock-Guttman B, Bakshi R. Gray and white matter brain atrophy and neuropsychological impairment in multiple sclerosis. *Neurology* 2006;**66**:685–92
38. Little AR, Benkovic SA, Miller DB, O'callaghan JP. Chemically induced neuronal damage and gliosis: enhanced expression of the proinflammatory chemokine, monocyte chemoattractant protein (MCP)-1, without a corresponding increase in proinflammatory cytokines(1). *Neuroscience* 2002;**115**:307–20